

LITHOGEOCHEMISTRY OF ULTRAMAFIC, GABBROIC AND TONALITIC ROCKS FROM THE NORTHEASTERN ARCHEAN ASHUANIPI COMPLEX, WESTERN LABRADOR: IMPLICATIONS FOR PETROGENESIS AND MINERAL POTENTIAL

T.S. van Nostrand
Regional Geology Section

ABSTRACT

The Ashuanipi Complex is a granulite-facies, sedimentary–plutonic subprovince of the Archean Superior Province, and is one of the largest high-grade gneiss terranes in Canada. In Labrador, the complex consists of older sequences of migmatitic paragneiss intercalated with pre-tectonic orthopyroxene-bearing tonalite to diorite, and subordinate gabbroic and ultramafic intrusions. These rocks predate the development of extensive metasedimentary diatexite, variably deformed granitoid intrusions and late granite pegmatite. Previous geochemical studies in the eastern Ashuanipi Complex indicate that the tonalite to diorite intrusions have tonalite–trondhjemite–granodiorite (TTG) or adakite-like affinities. The similar field associations, presence of relict igneous textures and anhydrous assemblages of the pre-tectonic granitoid and ultramafic rocks suggest there may be a genetic(?) relationship between these units. Preliminary lithogeochemistry for gabbroic and ultramafic rocks do not indicate a direct petrogenetic link. However, some similarities in trace- and rare-earth element abundances and behaviour suggest derivation from similar, silicate melt- and fluid-metasomatised mantle sources that yielded both felsic and mafic to ultramafic suites. This source metasomatic event may be related to subduction processes, however, the extent of crustal recycling in these rocks requires further isotopic investigations. The presence of anomalous base metals, including Ni, Cr, Ti and local Au and PGE in some gossan zones locally developed in tonalite and ultramafic sills, and coincident elevated lake-sediment concentrations, indicate a potential for similar mineralizing systems.

INTRODUCTION

Lithogeochemical investigations of rocks of the north-eastern Archean Ashuanipi Complex have been carried out in several studies (Morisset, 1988; Percival, 1991a, b; Percival *et al.*, 2003 and Schofield, 2014). These studies applied major-, trace- and rare-earth element analyses of the igneous and/or metasedimentary rocks, along with electron microprobe analyses of their constituent minerals. They included: i) determination of geothermobarometric conditions and the distinction of pre- and syn-metamorphic mineral assemblages (Morisset, 1988; Percival, 1991a; Schofield, 2014); ii) the nature of the protoliths and the evolution of supracrustal rocks, related migmatites and granitoid rocks (Percival, 1991b) and; iii) the classification of calc-alkaline ‘adakite-like’ igneous rocks of the complex in terms of a tectonic environment of formation (Percival *et al.*, 2003). Although geochemical data exists for the granitoid rocks and metasedimentary gneiss, only a few analyses have been reported for the mafic and ultramafic rocks of the region. Two B. Sc. undergraduate investigations focused on petrography and geochemical analysis of two distinct boudinaged ultramafic sills, one within the study area (Schofield, 2014)

and one in adjacent Québec (Morisset, 1988). Both projects attempted to classify the cumulate rocks and to provide an interpretation of metamorphic mineral assemblages and their P-T-X conditions of formation. Government and industry mineral assessment reports record local, elevated Au, Cu, Ni, Cr, Zn, Pd and Pt, hosted in altered zones found in ultramafic and gabbroic rocks (Percival, 1987; Thomas and Butler, 1987; Dimmell, 1989; Graves, 1992). This contribution classifies the ultramafic and mafic rocks and evaluates a possible petrogenetic relationship with the calc-alkaline, tonalitic granitoid rocks in the complex. The potential of these rocks to host Ni, Cu, Co, Au and platinum-group element (PGE) mineralization is also examined.

REGIONAL SETTING

The Superior Province is an Archean craton divided into two main domains, and these are further subdivided into several subprovinces (Card and Cielecki, 1986; Figure 1). Northern domain rocks are predominantly of continental affinity, have ages of between 2.75 and 2.65 Ga, and contain crustal vestiges as old as 3.0 Ga (Percival *et al.*, 2003). The southern domain contains linear, east–west-oriented,

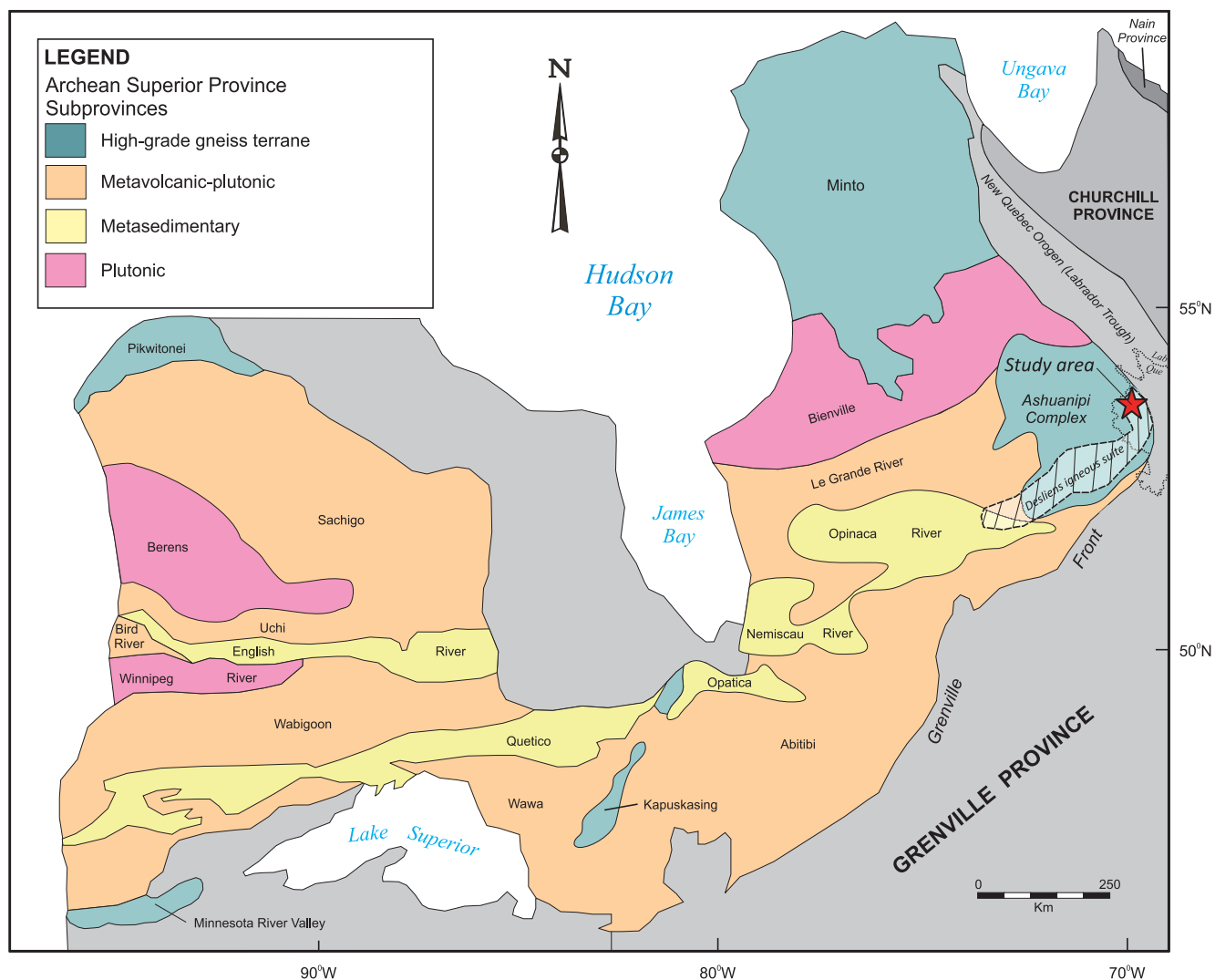


Figure 1. Subdivisions of the Superior Province, extent of the Desliens igneous suite (outlined by hashed lines) in the Ashuanipi and Opinaca River subprovinces (Percival *et al.*, 2003), and the location of the present study area (modified after Card and Cielecki, 1986).

metavolcanic-, metaplutonic- and metasedimentary-dominated subprovinces (Card and Cielecki, 1986). The metavolcanic subprovinces contain sequences of low-grade volcanic rocks intruded by tonalite to granite plutons (collectively termed ‘granite–greenstone’ terranes), whereas the metaplutonic subprovinces lack supracrustal rocks. Metasedimentary subprovinces comprise an approximately 2100-km-long belt, which stretches latitudinally across the southern Superior Province, and consist predominantly of metagreywacke sequences intruded by granite and tonalite. Most of the Superior Province formed between 3.0 and 2.65 Ga and the subprovinces are considered to demarcate amalgamated volcanic arcs, sedimentary prisms and composite terranes that were accreted progressively, from north to south between 2.75 and 2.70 Ga.

GEOLOGY OF THE ASHUANIPI COMPLEX

The Ashuanipi Complex is an Archean, granulite-grade subprovince of the eastern Superior Province, approximately 90 000 km² in area (Card and Ciesielski, 1986; Figure 1).

The oldest rocks in the complex are metasedimentary gneiss intruded by a 500-km-long belt of pre-tectonic tonalite, granodiorite, quartz diorite and diorite intrusions, referred to as the Desliens igneous suite (Percival, 1991a; Figure 1). Percival *et al.* (2003) interpreted these rocks as a contemporaneous fractionation series of intrusive rocks of tonalite–trondhjemite–granodiorite (TTG) (adakitic) affinity. Mafic and ultramafic rocks occur as isolated minor intru-

sions, sills, thin layers or dykes and have similar textures and field associations as the tonalite to diorite units. Leucogranite plutons are later intrusions that crosscut fabrics in other units. Pre-, to posttectonic granite, alkali-feldspar granite, alkali-feldspar quartz syenite veins, and syenogranite pegmatite also intrude most units. Granulite-facies metamorphism produced orthopyroxene-bearing assemblages and migmatitic fabrics and resulted in the production of predominantly sedimentary rock-derived, syn-, to late-metamorphic diatexite (Percival, 1991b; James, 1997). Percival (1987, 1991a, b) and Percival and Girard (1988) have described the regional geology of the Ashuanipi Complex in some detail, including the regional structural, metamorphic and geochronological relationships, and the reader is encouraged to consult these reports for additional information.

No age data has been reported from the immediate study area, but, several monazite and zircon U–Pb ages are available for comparable units in adjacent areas of Labrador and Québec. Pertinent geochronological data for the eastern Ashuanipi Complex are summarized below.

Summary of pertinent U–Pb geochronological data for the eastern Ashuanipi Complex

- 3.4 to 2.7 Ga: age range of detrital zircons from metasedimentary rocks; indicates that deposition of sedimentary rocks and minor volcanic rocks were completed by *ca.* 2.7 Ga (Mortensen and Percival, 1987)
- 2.72 Ga: intrusion of tonalite, granodiorite and diorite of the Desliens igneous suite (the analogous field relations and textures of the rocks of this suite and gabbro and ultramafic rocks within the study area may indicate a similar age (Percival *et al.*, 2003)
- 2.68 to 2.65 Ga: high-grade metamorphism, development of S_1 migmatitic fabric and intrusion of syn- to late-metamorphic garnet±orthopyroxene-bearing granite and granodiorite diatexite (Mortensen and Percival, 1987)
- 2.65 to 2.63 Ga: post peak metamorphic cooling (Percival *et al.*, 1988)
- 2.65 Ga: intrusion of posttectonic granite pegmatites and leucogranite (Percival *et al.*, 1991b)
- 2.65 to 2.6 Ga: post-metamorphic thermal event resulting in new zircon crystallization in diatexite and new monazite growth in older gneisses (Chevè and Brouillette, 1992)

ROCKS OF THE STUDY AREA

The location and extent of the Ashuanipi Complex and the study area, with respect to the other tectonic provinces of Labrador are illustrated in Figure 2. The geology of the

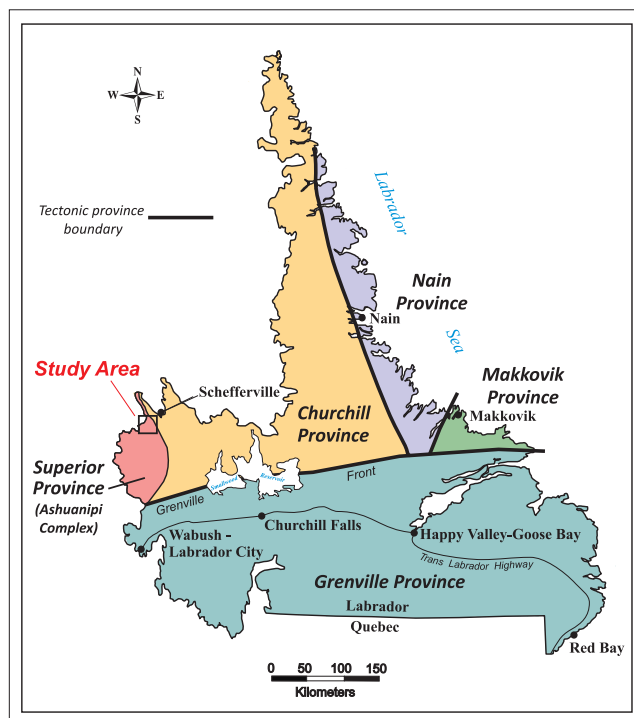


Figure 2. Location of the study area and the extent of the Ashuanipi Complex, with respect to the tectonic provinces of Labrador (modified from van Nostrand and Bradford, 2014).

Ashuanipi Complex is shown in Figure 3 and is discussed in detail by van Nostrand and Bradford (2014). The rocks include older migmatitic metasedimentary gneiss intruded by pre-tectonic, foliated to gneissic tonalite, granodiorite and diorite intrusions comparable to those of the Desliens igneous suite (Percival, 1991a). Gabbro and pyroxene-rich ultramafic rocks occur as small intrusions, boudinaged sills and layers. Percival *et al.* (2003) suggested these rocks may have a petrogenetic relationship with rocks of the Desliens igneous suite, however, he noted that the inclusion of the gabbro and ultramafic rocks in this suite is problematic, as compositions intermediate between diorite and the gabbro–ultramafic rocks were not observed. Granite to granodiorite diatexite is the dominant rock type, occurring as 10s of km-scale bodies and as abundant, outcrop-scale, syn- to late-tectonic veins and fabric concordant layers. Late syn- to posttectonic granite and alkali-feldspar quartz-syenite pegmatite veins intrude most units. Granulite-facies conditions are inferred throughout the map area, based on widespread orthopyroxene–garnet–melt assemblages in the migmatitic gneiss units, but some granitoid and ultramafic rocks preserve remnants of primary pyroxene (Percival, 1991a; Schofield, 2014). Evidence of upper amphibolite to local greenschist-facies retrograde metamorphism is noted by secondary alteration of pyroxene, olivine and plagioclase.

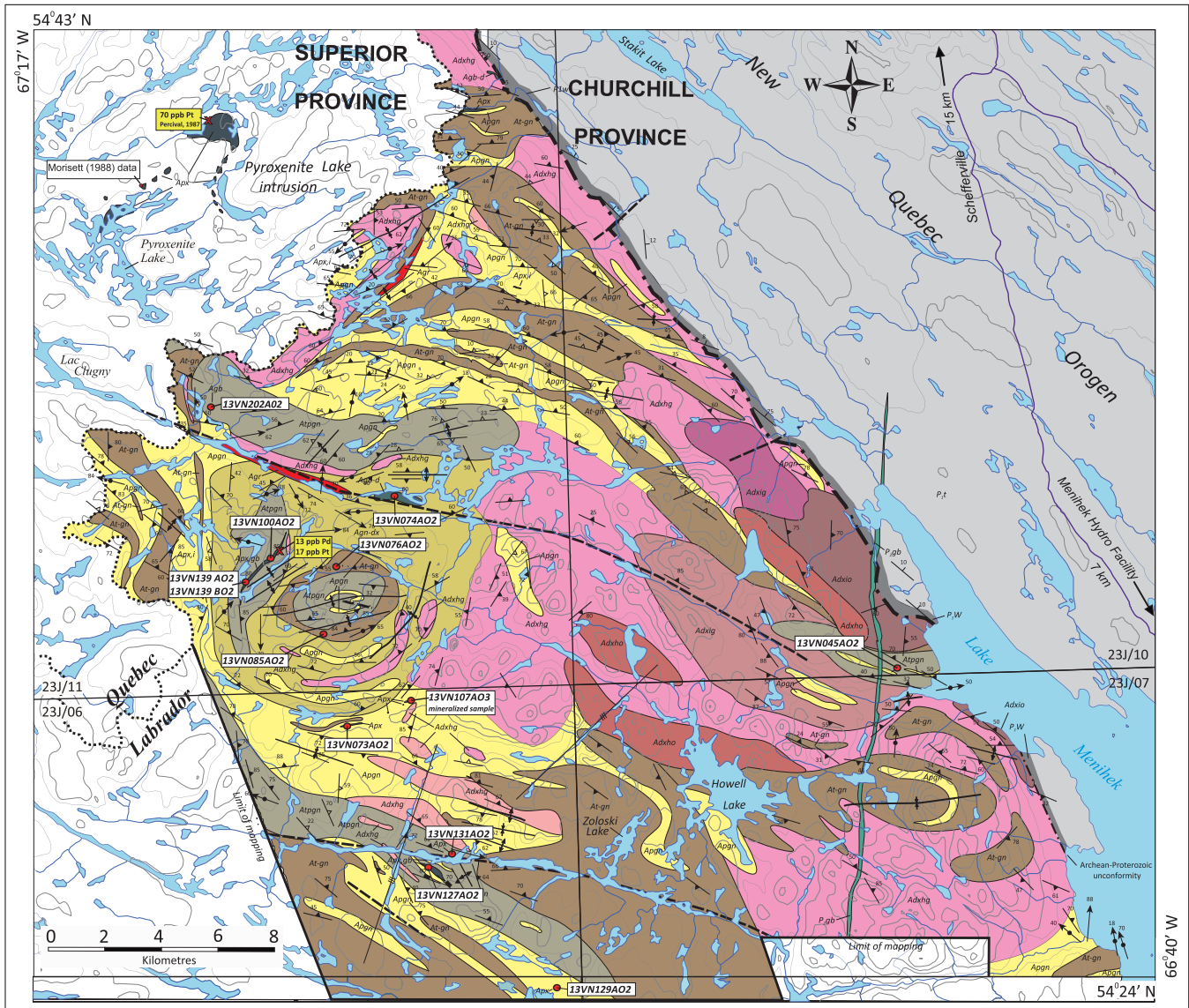


Figure 3. Geology of the study area from van Nostrand and Bradford (2014). See van Nostrand and Bradford (2014) for a more detailed map. Rocks interpreted as the Desliens igneous suite area are included in Unit At-gn (tonalite to diorite). The mafic-ultramafic rocks include Agb-d (gabbro-diorite), and Apx (pyroxenite). Locations of samples listed in Table 1 are shown. The locations of the samples of Percival et al. (2003) used in this study are not shown. Location of the Pyroxenite Lake intrusion is after Percival (1993).

Several mineral occurrences with variable but elevated Au, Cu, Cr and Ni values are hosted in gossanous, migmatitic gneiss, foliated granitoid rocks, gabbro, ultramafic rocks and local lenses of oxide-facies iron formation. Most of these occurrences have only been investigated on a cursory basis.

DESCRIPTION OF ROCK UNITS

The lithogeochemical samples investigated herein were obtained from three distinct rock units and each of these are briefly summarized below. More complete descriptions of

these rocks are presented in Percival (1987, 1991a) and van Nostrand and Bradford (2014) and the reader is referred to these reports for a more complete synthesis of these and other rock types of the region.

UNIT At-gn – FOLIATED TO GNEISSIC TONALITE, GRANODIORITE AND DIORITE

This unit consists predominantly of tonalite but includes granodiorite, quartz diorite and diorite. The rocks vary from white-, green-, brown- and grey-weathering, fine to coarse grained and massive to gneissic. The dominant

LEGEND

Neoproterozoic ?

P₂gb Green- to grey-weathering, gabbro to diabase dyke

Adxo Heterogenous, orthopyroxene-dominant diatexite; migmatitic gneiss; foliated granitoid rocks

Agb Weakly foliated to massive, biotite + orthopyroxene ± clinopyroxene gabbro, gradational to diorite

Paleoproterozoic

New Québec Orogen (Labrador Trough)

P₁t Undifferentiated sedimentary and igneous rocks of the New Québec Orogen (Labrador Trough)

Apx Dark-green- to black-weathering, weak to strongly foliated, locally layered ultramafic sills. Sills are composed primarily of pyroxenite, with local, m-scale layers of websterite, harzburgite and melagabbro and gabbro

P₁w Wishart Formation. Metamorphosed quartz arenite, arenite, siltstone, shale and black chert

At-gn Grey-, white-, brown-, to cream-weathering, massive to gneissic orthopyroxene-bearing tonalite, granodiorite, quartz diorite and minor diorite (Desliens igneous suite)

Archean

Agr Homogeneous, medium-grained, weak to moderately foliated biotite ± hornblende leucogranite

Agn-dx Foliated to gneissic migmatitic metasedimentary gneiss; heterogeneous and homogeneous, garnet-dominant diatexite

Adxhg Homogeneous, garnet-dominant diatexite; migmatitic gneiss; foliated granitoid rocks

Atpgn Foliated to gneissic tonalite to granodiorite migmatitic gneiss; migmatitic metasedimentary gneiss

Adxho Homogeneous, orthopyroxene-dominant diatexite; migmatitic gneiss; foliated granitoid rocks


Apgn White-, cream-, honey-brown-, dark-brown-, to grey-weathering, garnet+biotite+orthopyroxene migmatitic metasedimentary gneiss


Adxig Heterogeneous, garnet-dominant diatexite; migmatitic gneiss; foliated granitoid rocks


Symbols


 Provincial boundary


 Geological contact (approximate or assumed)

 Bedding attitude. Common in sedimentary rocks of the Wishart Formation. Rare bedding preserved in migmatitic gneiss is observed in one locality


 Local, primary igneous layering in mafic and ultramafic rocks. Defined by cm to m-scale layers of variation in mineral proportions


 S₁ gneissosity defined by alternating leucocratic and melanocratic layers in migmatitic gneiss, commonly accentuated by concordant and near-concordant injected granitoid rock veins

 S₂ foliation defined primarily by preferred alignment of mafic minerals in tonalite, diatexite, variably deformed granitoid rocks and mafic and ultramafic rocks

 Second generation, minor F₂ fold axis plunge direction. Developed predominantly in migmatitic gneiss, diatexite and coarse granite and alkali-feldspar granite veins


 Second generation, L₂ lineation plunge direction defined by aligned minerals or slicken striae


 Brittle to ductile fault structure. Defined, in part, by brittle fault breccia and ductile features including lineations, asymmetric structures and rare C-S fabric relationships

 Unconformity between Archean migmatitic gneiss and siliciclastic rocks of the Paleoproterozoic New Quebec Orogen (Labrador Trough)

 Synform structure (plunge undetermined)

 Antiform structure (plunge undetermined)

 Air photograph lineament

 13VN100AO2 Location of sample numbers used in this study (Tables 1 and 2)


 13 Pd, 18 Pt Location of elevated Pt and Pd assay from a pyroxenite sill reported by Graves (1992)

Figure 3. Legend.

mineral assemblage is orthopyroxene ± clinopyroxene ± biotite ± garnet ± amphibole. van Nostrand and Bradford (2014) noted the absence of a leucosome component in the foliated tonalite and interpreted these rocks as less-deformed equivalents of the migmatitic gneiss (Plates 1 and 2).

UNIT Agb – GABBRO

Mafic rocks range from gabbro to leucogabbro and locally to olivine gabbro and occur as rare, small plutons and thin sills within the gneisses as well as cm- and m-scale layers within large ultramafic sills. The largest gabbro body is in the north-central study area, exposed along a southeast-



Plate 1. *Medium-grained, massive to weakly foliated tonalite of the Desliens igneous suite. Irregular brown patches are sieve-textured, inclusion-rich orthopyroxene, interpreted as relict igneous oikocrysts.*



Plate 2. *Fine-grained, stromatic-textured, orthopyroxene-bearing migmatitic tonalite gneiss of the Desliens igneous suite. This rock is interpreted as a gneissic equivalent of the massive to foliated, oikocrystic tonalite shown in Plate 1.*

striking fault (sample 13VN074A02, Figure 3). In the north-western area, a foliation-concordant, 30-m-wide gabbro to melagabbro sill intrudes metasedimentary gneiss (sample 13VN202A02, Figure 3). These rocks consist of orthopyroxene, clinopyroxene, hornblende, plagioclase, spinel and magnetite, and exhibit local relict igneous layering (Plate 3).

UNIT Apx – PYROXENE-RICH ULTRAMAFIC ROCKS

Ultramafic rocks are subordinate in the study area, occurring as foliation/gneissosity parallel, elongate bodies up to 200 m thick and 1.5 km long and, more commonly, as



Plate 3. *Medium-grained, equigranular gabbro comprising a 30-m-thick sill intruding metasedimentary gneiss in the western study area (Sample 13VN202A02). The gabbro contains orthopyroxene, clinopyroxene, plagioclase and minor amphibole and magnetite. A weak, local compositional layering can be observed.*

10s of m-scale, layers and boudins that occur in metasedimentary gneiss and foliated or gneissic granitoid rocks (Figure 3). They range from primarily pyroxenite to harzburgite, olivine melagabbro, melanorite and lherzolite. The mineral assemblages of these rocks include variable proportions of hypersthene and bronzite, diopside, olivine, hornblende, plagioclase, biotite, spinel, magnetite and apatite, in relative decreasing abundance. The extent of alteration varies, depending on the dimensions of the sill, the rock type and the position of various layers within individual intrusions. The rocks exhibit a variety of textures, ranging from massive and locally layered with very coarse-grained pyroxene phenocrysts (oikocrysts?), to fine grained, recrystallized and strongly foliated (Plates 4 and 5). The protolith(s) of these rocks is equivocal, but their elongate and tabular shape, concordant and sharp contacts and rare chilled margins against the enclosing rocks, suggest they are sills. Igneous layering was noted in several areas and is defined by diffuse to sharp variations in the proportions and grain size of constituent minerals, in particular pyroxene and plagioclase (Plate 6). The layering suggests that these rocks are likely cumulate in origin.

One of the largest ultramafic bodies is located in the west-central part of the study area (samples 13VN100A02, 13VN139A02 and 13VN139B02, Figure 3). The intrusion is approximately 150 m thick and 1.5 km long and consists predominantly of coarse-grained, foliated pyroxenite, grading to olivine gabbro, melagabbro, harzburgite and minor dunite. The pyroxenite (sample 13VN139A02) appears to be truncated at a low angle by a later, massive to weakly foliated, fine-grained intrusion (sample 13VN139B02, Plates 7



Plate 4. Strongly foliated, medium-grained, homogenous pyroxenite of the large ultramafic sill in the western study area (sample 132VN100A02). This contains local, thin serpentinite veins parallel to the fabric.



Plate 5. Massive to weakly foliated, porphyritic pyroxenite of the ultramafic sill in the southern study area (sample 13VN127A02). Orthopyroxenes (grey-green-weathering crystals) are interpreted as relict igneous oikocrysts. White patches are lichen-covered oikocrysts.

and 8), and indicates more than one generation of ultramafic magma may be present.

In the southern part of the study area, several, massive to strongly foliated ultramafic lenses occur in metasedimentary gneiss. The largest is a 200-m-thick by 800-m-long body consisting of pyroxenite, harzburgite and melagabbro and melanorite, with local igneous layering (Figure 3, sample 13VN127A02). Schofield (2014) carried out detailed petrographic, scanning electron microscope-mineral liberation analyses (SEM–MLA) and electron probe microanalyses (EPMA) of this sill. Schofield (*op. cit.*) reported the



Plate 6. Relict, olivine-rich igneous layering preserved in a weak to moderately foliated pyroxenite to websterite layer in a large boudinaged sill in the southern study area.



Plate 7. Strong foliation in dark-weathering pyroxenite (Unit Apx: sample 13VN139A02) that is truncated at a low angle, by a fine-grained, weakly foliated ultramafic intrusion that may be a dyke (sample 13VN139B02).

presence of preserved relict igneous textures and mineral phases in this sill that have been chemically homogenized during regional granulite-upper amphibolite-facies metamorphism and subsequent retrogression to amphibolite and locally greenschist-facies assemblages.

LITHOGEOCHEMISTRY

ANALYTICAL METHODS

Samples collected for this study were analyzed for major and trace elements at the Geochemical Laboratory, Department of Natural Resources, Government of Newfoundland and Labrador, Howley Building, Higgins Line,

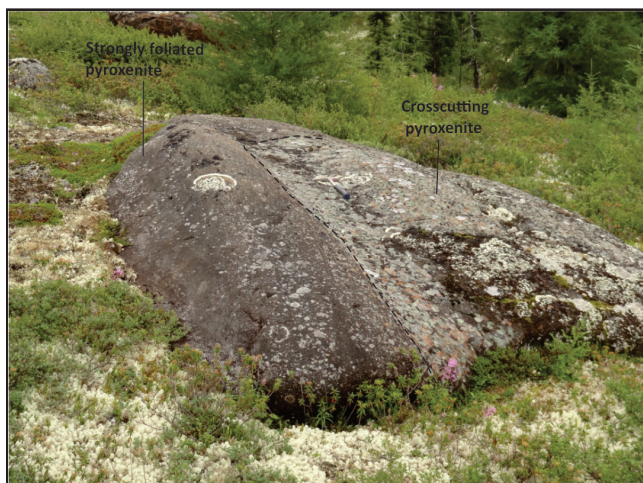


Plate 8. Larger view of the two intrusive ultramafic rocks shown in Plate 7. The apparent fold hinge in the upper part of photograph suggests that both intrusions were emplaced prior to the regional folding event.

St. John's. Powdered rock samples were fused at 1000° C in a graphite crucible for 30 minutes using a Lithium Borate mixture. The molten fusion bead was poured directly into a 10% solution of nitric acid and stirred for about 15 minutes until dissolution. The solution was then topped up to a final volume of 100 ml. This solution was measured directly by Thermo Instruments iCap 6500 Inductively Coupled Plasma Optical Emission Spectrometer (ICP-OES) for major- and trace-element contents (SiO₂%, Al₂O₃%, Fe₂O₃ Total %, MgO%, CaO%, Na₂O%, K₂O%, TiO₂%, MnO%, P₂O₅%, Cr ppm, Zr ppm, Ba ppm). The analyte solution was diluted to 20% of the original and made to volume with two percent nitric acid. Trace-element abundances were measured by a Thermo Instruments X-Series II Inductively Coupled Plasma Mass Spectrometer (ICP-MS: V, Co, Ga, Ge, Sr, Y, Nb, Mo, Cd, Sn, Cs, REE, Hf, Ta, W, Tl, Bi, Th and U: all in ppm). Analytical methods for FeO and LOI are after Finch (1998). The trace elements Au and Ta were analyzed at Becquerel Laboratory in Mississauga, Ontario by using Neutron Activation (Method BQ-NAA-1, www.Becquerellabs.com).

SAMPLE SELECTION

A total of thirteen lithochemical analyses are presented, including six samples of relatively unaltered pyroxenite, one sample of a crosscutting pyroxenite, one mineralized pyroxenite, two gabbro (one from a thin, concordant sill and one from a small pluton) and, three samples of tonalite, ranging from weakly foliated to gneissic. These are supplemented by fourteen analyses of rocks of the Desliens igneous suite from the eastern Ashuanipi Complex (Percival *et al.*, 2003) for comparison with the tonalities collected in

this investigation. The major-element data for six samples of ultramafic rocks from the Pyroxenite Lake intrusion (Figure 3; Morisset, 1988) are also included to compare with the general bulk composition of pyroxenite sills in the study area. These data may collectively help to indicate if a petrogenetic relationship exists between all of the rocks of this suite, including the gabbro and the ultramafic rocks (*e.g.*, Percival, 1991a).

Most ultramafic and gabbro samples used in this study were collected from relatively unaltered, fine- to medium-grained marginal zones of the sills and contain no visible mineralization. Tonalite samples are representative of the intrusion from which they were collected.

LITHOCHEMISTRY RESULTS

Sample descriptions and UTM coordinates are given in the Appendix, and the locations are indicated on Figure 3. Major-element-oxide and trace-element data for the ultramafic rocks, gabbro and tonalite from the study area are shown in Table 1. Note that the mineralized pyroxenite sill (sample 13VN107A03) is not included on most of the following discrimination diagrams but is only plotted on a primitive mantle-normalized extended trace-element diagram and a rare-earth element (REE) plot (Figure 11A, B) and discussed in terms of the base- and rare-element mineralization potential of these rocks.

Major-Element Geochemistry

Field characteristics of the ultramafic rocks, gabbro and tonalite are supported by their bulk chemical compositions as shown on a Jensen (1976) plot, a modified Irvine and Baragar (1971) AFM diagram and a total alkali-silica plot after Le Bas *et al.* (1986) in Figure 4A–C. The major-oxide data of Morisset (1988) from the Pyroxenite Lake intrusion are also included on these three diagrams for comparison with the bulk compositions of ultramafic rocks from this study. However, the samples from the intrusion in Québec were collected from several different horizons in a layered ultramafic sill and are not therefore representative of the intrusion margins. The legend for the samples shown with these figures is applicable for all discrimination diagrams used in this study. The trace-element and REE plots (Figure 11A–F) have a different legend.

Figure 4A shows that all of the ultramafic rocks and the gabbro sill plot in a relatively tight cluster in the basaltic komatiite field, following a komatiite trend, whereas the gabbro from the small pluton plots as a Mg-rich tholeiite. The tonalites fall within the tholeiite and dacite-andesite fields, roughly following a calc-alkaline-like trend.

Table 1. Major-oxide and trace-element analyses for samples used in this study. All analyses (except Au, Mo and Ta) were performed at the Newfoundland Department of Natural Resources, Geological Survey Laboratory. Methods for FeO and LOI after Finch (1998). Au and Ta were analyzed using Method BQ-NAA-1, (www.Bequerellabs.com). All other elements analyzed using methods described in Analytical Methods section in text. Negative sign indicates below detection limit

	13VN073 AO2 Pyroxenite massive	13VN100 AO2 Pyroxenite foliated	13VN127 AO2 Pyroxenite porphyritic	13VN129 AO2 Pyroxenite foliated	13VN131 AO2 Websterite foliated	13VN139 AO2 Pyroxenite foliated	13VN139 BO2 Pyroxenite later intrusion?	13VN074 AO2 Gabbro small pluton	13VN202 AO2 Gabbro sill	13VN045 AO2 Tonallite gneiss	13VN076 AO2 Tonallite massive	13VN085 AO2 Tonallite foliated
SiO2	46.00	44.23	50.47	47.07	50.48	41.89	49.23	48.63	43.33	64.44	66.83	60.30
Al2O3	7.86	6.75	6.54	8.67	8.75	7.63	6.65	13.12	10.48	16.88	14.60	17.42
Fe2O3t	9.96	10.50	9.16	10.37	9.40	11.44	9.89	11.20	12.53	4.12	4.58	7.16
FeO	7.05	4.18	2.73	0.54	1.69	4.31	0.19	4.31	0.80	0.93	0.77	1.81
MgO	22.38	24.72	24.92	18.99	20.89	6.42	8.73	8.90	10.44	2.99	3.43	4.82
CaO	7.62	6.90	5.51	10.01	4.18	23.81	23.93	11.45	20.51	1.93	2.73	4.15
Na2O	0.47	0.26	0.46	0.50	0.70	0.11	0.70	1.18	0.58	4.48	3.00	1.73
K2O	0.12	0.04	0.23	0.15	1.13	0.49	0.36	0.89	0.26	1.61	2.76	2.87
TiO2	0.385	0.333	0.308	0.451	0.335	0.395	0.300	0.766	0.585	0.494	0.484	0.827
MnO	0.147	0.169	0.137	0.173	0.153	0.172	0.152	0.194	0.175	0.062	0.058	0.075
P2O5	0.044	0.026	0.112	0.017	0.151	0.024	0.026	0.059	0.045	0.068	0.145	0.076
LOI	3.39	5.52	1.14	1.64	2.26	5.87	1.12	1.21	3.05	1.36	0.65	1.74
Total	98.39	99.45	98.99	98.05	98.43	98.57	98.15	99.78	98.00	99.12	99.06	98.88
Mg#	84	85	86	81	84	85	85	70	79	52	58	57
V	149.40	142.30	103.10	189.70	119.50	173.80	139.30	274.20	212.10	101.00	85.80	146.60
Co	86.93	88.31	84.05	94.83	71.84	95.39	85.48	57.31	83.14	16.19	15.50	21.17
Ga	10.26	7.68	9.05	11.14	12.28	7.95	9.13	17.26	14.07	21.95	18.06	24.97
Ge	3.37	2.42	2.78	3.43	4.96	3.10	3.26	3.10	4.59	3.27	2.71	3.66
Sr	43.06	34.10	79.56	182.30	119.90	99.40	37.24	139.50	48.12	386.90	671.70	282.60
Y	8.63	8.04	6.82	10.58	11.91	10.41	7.39	19.95	14.62	12.40	6.83	12.14
Nb	1.45	0.76	2.40	1.41	2.94	1.01	0.94	2.89	1.40	5.11	4.25	8.62
Mo	-2.00	-2.00	-2.00	-2.00	-2.00	-2.00	-2.00	-2.00	-2.00	-2.00	-2.00	-2.00
Cd	-0.20	-0.20	-0.20	-0.20	-0.20	-0.20	-0.20	-0.20	-0.20	-0.20	-0.20	-0.20
Sn	1.85	-1.00	1.46	4.62	3.08	-1.00	8.08	0.97	3.23	-1.00	0.77	-1.00
Cs	-0.50	0.70	-0.50	-0.50	4.33	1.03	0.56	0.51	-0.50	-0.50	0.81	2.71
La	4.48	1.74	9.97	3.57	12.78	4.33	2.70	7.03	4.23	33.95	29.90	30.90
Ce	9.11	2.77	19.04	6.16	30.20	4.33	3.57	13.70	7.41	60.78	54.57	61.23
Pr	1.19	0.39	2.30	0.85	4.15	0.63	0.42	1.86	0.98	6.48	5.91	7.10
Nd	5.27	1.98	9.97	3.87	17.58	3.22	2.34	8.61	5.18	23.31	21.77	26.41
Sm	1.40	0.71	1.99	1.20	3.38	1.04	0.74	2.44	1.59	3.31	3.15	4.52
Eu	0.40	0.26	0.54	0.39	0.74	0.35	0.16	0.81	0.50	1.22	1.06	1.34
Tb	0.25	0.18	0.23	0.27	0.43	0.24	0.18	0.54	0.38	0.37	0.26	0.51
Gd	1.49	1.11	1.66	1.62	2.94	1.48	1.04	3.13	2.24	2.48	2.11	3.43
Dy	1.66	1.37	1.36	1.91	2.35	1.74	1.16	3.43	2.44	2.23	1.28	2.54
Ho	0.31	0.28	0.24	0.39	0.43	0.36	0.26	0.74	0.54	0.45	0.25	0.42
Er	0.98	0.87	0.74	1.21	1.23	1.11	0.84	2.30	1.65	1.36	0.71	1.05
Tm	0.14	0.11	0.10	0.16	0.16	0.11	0.11	0.32	0.23	0.20	0.08	0.12
Yb	0.86	0.81	0.69	1.17	1.20	1.01	0.76	2.16	1.57	1.36	0.65	0.82
Lu	0.15	0.12	0.11	0.15	0.16	0.17	0.11	0.31	0.24	0.24	0.09	0.15
Hf	1.06	0.61	1.37	1.02	2.20	0.77	0.71	1.65	1.21	4.06	3.47	3.02
Ta	0.40	-0.20	-0.20	0.30	-0.20	-0.20	-0.20	-0.20	-0.20	0.30	0.60	0.50
W	-1.00	-1.00	-1.00	-1.00	-1.00	-1.00	-1.00	-1.00	-1.00	-1.00	-1.00	-1.00
Tl	-0.10	-0.10	-0.10	-0.10	-0.10	-0.10	-0.10	-0.10	-0.10	0.13	0.21	0.30
Bi	0.53	-0.40	-0.40	-0.40	-0.40	-0.40	-0.40	-0.40	-0.40	-0.40	-0.40	-0.40
Th	0.72	-0.10	1.54	0.30	0.87	0.17	0.48	1.23	0.56	7.28	4.66	8.52
U	0.19	-0.05	0.49	0.07	0.25	-0.05	0.19	0.15	0.22	0.30	0.74	1.02
Zr	36.4	21.7	43.5	31.2	47.9	26.6	19.8	47.5	41.5	139.2	126.8	104.2
Au	2.00	1.00	10.00	-1.00	2.00	12.00	4.00	-1.00	11.00	-1.00	6.00	-1.00
Cr	1801	2042	1771	1615	1801	2136	1801	682	1882	115	174	200
Ba	1.81	4.19	5.15	20.92	150.24	50.3	4.3	116.3	13.2	500.2	1313.9	824.4
Ni	745	785	858	734	740	807	837	214	639	42	56	67
Ti	2401	1999	1940	2740	2119	2453	1908	4736	114	2821	2925	4243

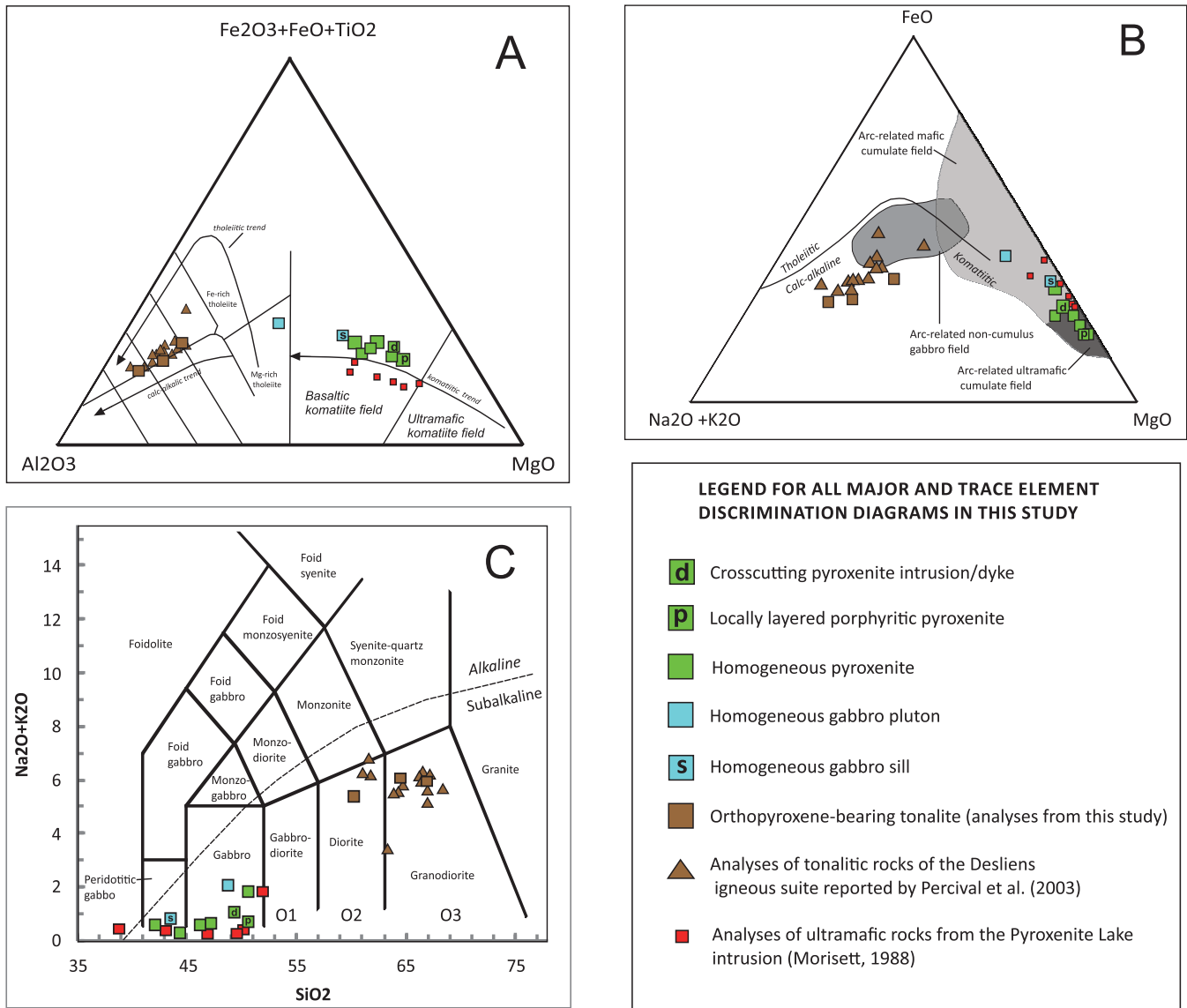


Figure 4. A) Al_2O_3 -Fe-Ti-oxide-MgO diagram (Jensen, 1976) showing komatiitic, tholeiitic and calc-alkaline trends; B) AFM discrimination plot (Irvine and Baragar, 1971; with fields after Beard, 1986) showing the MgO-rich pyroxenite and gabbro versus the apparent calc-alkaline tonalites. Also shown are arc-related mafic-ultramafic fields and the tholeiite-calc-alkaline divide; and C) Na_2O+K_2O versus SiO_2 (TAS) diagram after Le Bas et al. (1986) with plutonic rock nomenclature after Middlemost (1985).

In Figure 4B, most ultramafic rocks plot in a tight group within, or on the boundary of, the arc-related, Mg-rich ultramafic cumulate field. One pyroxenite and the gabbro sill plot in the Mg-rich mafic cumulate field, whereas the gabbro pluton is has a slightly more Fe-rich mafic cumulate-like composition. The tonalite samples all plot within the calc-alkaline field. The data from the Pyroxenite Lake intrusion (Morisett, 1988) plot primarily within the mafic cumulate field.

A total alkali vs silica (TAS) diagram (Le Bas et al., 1986) is shown in Figure 4C where most pyroxenites and the

gabbro pluton are low alkali gabbros and two pyroxenites and the gabbro sill are peridotitic gabbros. The data from the Pyroxenite Lake intrusion (Morisett, 1988) span both the low alkali gabbroic and peridotitic gabbro fields. The tonalite samples are predominantly granodiorite with a few samples yielding diorite and monzonite compositions.

All of the relatively unaltered ultramafic rocks have high MgO (18.98–24.92 wt. %) and Mg# (81-86), low and restricted TiO_2 (0.3-0.45 wt. %) and significant variation in loss on ignition (LOI = 1.14-5.87 wt. %). The mineralized pyroxenite sill has a comparatively low MgO content (8.38

wt. %) and Mg# (49), with higher TiO₂ (0.66 wt. %) and a high LOI (5.54 wt. %). The two gabbro samples have moderate MgO (6.46–11.09 wt. %) and Mg# (70–79). Tonalites have modest ranges in MgO (1.93–4.15 wt. %) and Mg# (52–58), relatively high but still low TiO₂ (0.48–0.82 wt. %) and low LOI (0.65–1.74 wt. %).

Compositional trends for the major elements in all rocks are illustrated in Figure 5A–F. The relatively incompatible element oxide MgO was used as a fractionation index. The gabbro and ultramafic rocks show weak inverse correlations between Na₂O and Al₂O₃ and MgO, whereas Fe₂O₃^T increases with MgO content is apparent in Figure 5D. SiO₂ (43–50 wt. %), K₂O (0.04–1.13 wt. %) and P₂O₅ (0.017–0.112 wt. %) have wide compositional ranges and do not show any apparent correlation with MgO. Major oxide trends for the tonalitic rocks indicate that Fe₂O₃^T and P₂O₅ positively correlate with MgO, whereas SiO₂ (60.3–68.3 wt. %) and Al₂O₃ (14.6–17.2 wt. %) exhibit negative correlations. Ranges of K₂O (0.63–2.73 wt. %) show no obvious correlation with MgO. The three tonalites from this study are very similar overall to those of Percival *et al.* (2003).

Trace-Element Geochemistry

Ultramafic rocks, gabbros, and tonalites show enrichment in both the incompatible and compatible trace elements. Depending on the relative element compatibility, a range of trace-element behaviour *versus* the immobile element Zr, is evident in Figure 6A–F. For the gabbro and ultramafic rocks, the incompatible elements Th, Nb, La and Y show a positive correlation with Zr. The transitional element Ni exhibits a relatively small range of values of 639–858 ppm, with the exception of the sample of the gabbro pluton (214 ppm Ni) and shows a very weak negative relationship with Zr. The trace-element characteristics of the tonalitic rocks (including the data of Percival *et al.*, 2003), show a wide scattering of both incompatible and compatible elements. No apparent relationship of Th, La and Ni with Zr is evident, whereas Nb, Y and Yb show weak positive correlations *versus* Zr.

A TiO₂ vs Zr plot showing the discrimination fields after Hallberg (1985) is presented in Figure 7. The ultramafic rocks plot in a tight group straddling the low TiO₂ komatiite basalt and andesite or komatiite basalt fields. The gabbro samples are both komatiitic basalts. Most of the tonalite samples plot as andesites, with a few analyses indicating transitional andesite–komatiite basalt compositions.

Bivariate ratio discrimination diagrams may provide a more reliable means to identify the affinity of the rocks because they apply ratios of trace elements that are considered immobile during alteration and metamorphism (*e.g.*, Nb, Th, Yb, Zr and TiO₂). The trace-element ratio diagrams

are based primarily on the identification and utilization of geochemical parameters for specific magmatic affinities and petrogenetic processes as well as overall better performance (Pearce, 2008).

Figure 8 shows a Zr/Y vs Th/Yb plot (Winchester and Floyd, 1977, modified by Ross and Bedard, 2009). The two gabbro samples and most ultramafic rocks span the tholeiite field and the tholeiite–calc-alkaline transitional field whereas the porphyritic pyroxenite and the tonalites plot in the calc-alkaline field. Figure 9A and B are two discrimination diagrams that distinguish TTG (adakites) and classical arc-related rock. In the La/Yb vs Yb diagram (Figure 9A: Drummond and Defant, 1990) the tonalites and one pyroxenite span the low Y range of the TTG field, and one pyroxenite plots in the transitional arc–related to adakite field. All other pyroxenites and the two gabbros have very low La/Yb ratios and plot outside these fields. Although not labelled on this diagram, the low La content of the latter rocks would suggest these are of arc-like and transitional to tholeiite. In a Sr/Y vs Y plot (Figure 9B: Castillo, 2006), only one tonalite from this study yielded a TTG-like composition whereas most of the tonalite samples of Percival *et al.* (2003) fall within or just outside of this field. One tonalite and the gabbro pluton are arc-related, dacite–andesite–rhyolites. All ultramafic rocks, the gabbro sill and two tonalites have low Y/Sr ratios and plot outside these fields, features characteristic of rocks transitional between arc-like and tholeiite in composition.

The enrichment of Th, relative to equally incompatible Nb, provides an effective proxy of crustal input into mafic, mantle-derived rocks (Pearce, 2008). Volcanic-arc basalts, with crustal input *via* subduction, plot parallel to the mid-ocean ridge basalt (MORB) array at higher Th/Nb, whereas lithospheric contamination or deep asthenospheric recycling produces trends that are above, and oblique to the MORB array. All of the samples from the study have Th/Nb higher than the MORB array (Figure 10), indicating an intraoceanic, volcanic-arc setting whereby subduction zone fluids contributed Th in their petrogenesis (Pearce, 2008). The gabbro–ultramafic rocks and the tonalitic rocks form distinct groups that approximately parallel the MORB array, implying that the parental magmas to these rocks were contaminated by a lithospheric or crustal component, likely *via* subduction processes. However, an apparent slight obliquity in the trend of the gabbro and ultramafic rocks with respect to the MORB array (Figure 10) may suggest some contamination of the source magma

Rare-Earth Element (REE) and Extended Multi-Element Diagrams

Chondrite-normalized REE and primitive mantle-normalized multi-element diagrams (Sun and McDonough,

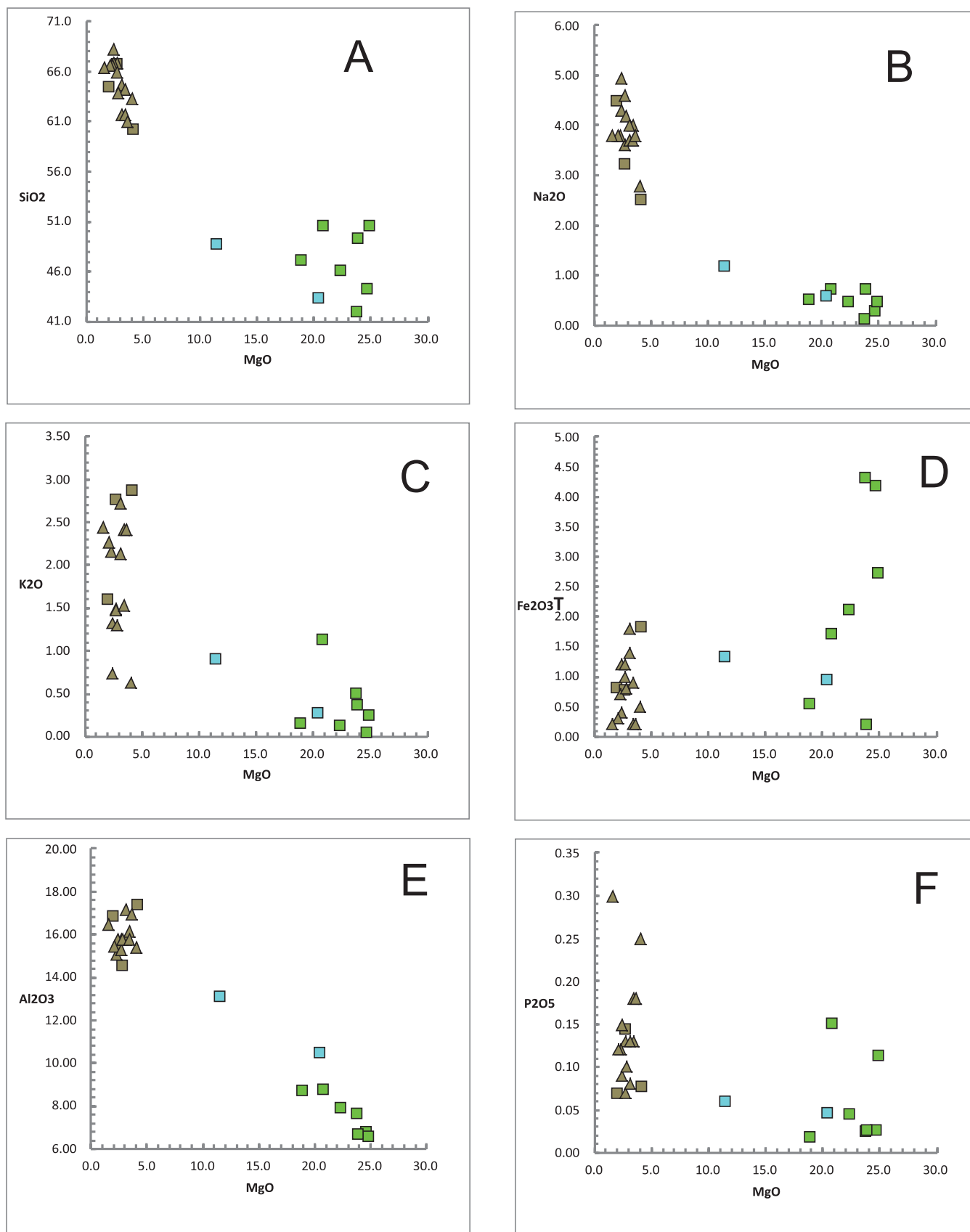


Figure 5A–F. Major-element oxide versus MgO diagrams for the rocks of the region. Symbols as in Figure 4.

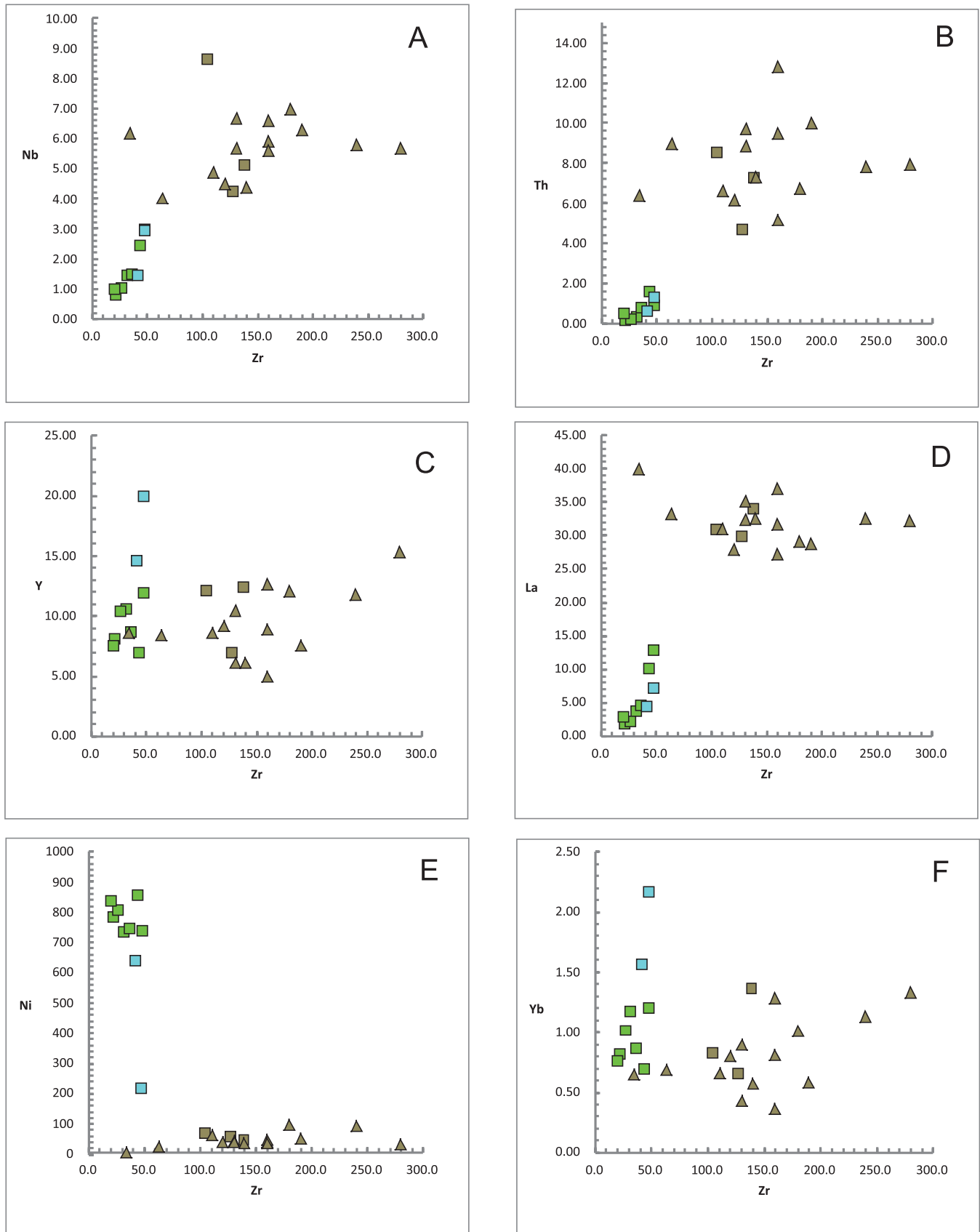


Figure 6A–F. Selected compatible and incompatible trace elements plotted against Zr for the rocks of the region. Symbols as in Figure 4.

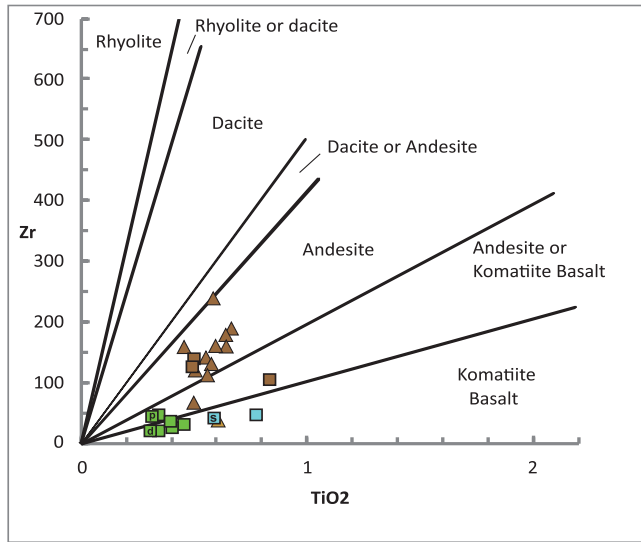


Figure 7. TiO_2 vs Zr plot with compositional fields after Hallberg (1985). Symbols as in Figure 4.

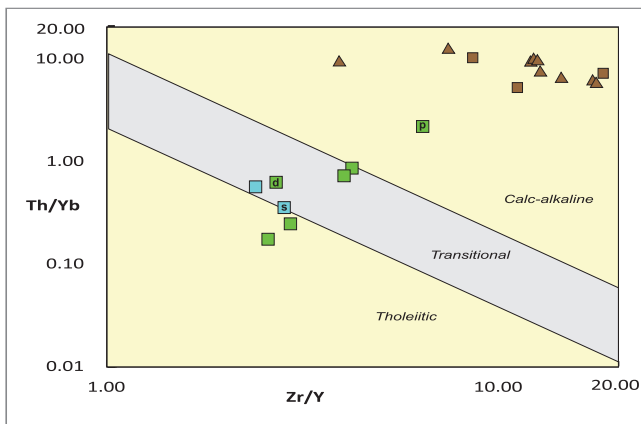


Figure 8. Th/Yb vs Zr/Y -discrimination diagram (Winchester and Floyd, 1977) showing tholeiitic, transitional and calc-alkaline fields as modified by Ross and Bedard (2009). Symbols as in Figure 4.

1989) are shown for the ultramafic, gabbroic and tonalitic rocks in Figure 11A–F. The ultramafic rocks exhibit variable and weakly light-REE enrichment, and flat heavy-REE profiles (Figure 11A). The crosscutting, fine-grained pyroxenite and the porphyritic pyroxenite have minor negative Eu anomalies. The multi-element profiles of the ultramafic rocks (Figure 11B) show significant scattering of the highly and moderately incompatible elements (to the left of Eu) with very consistent mantle compatible element contents (to the right of Eu). All pyroxenites exhibit moderate Nb and Ti troughs, whereas two samples (the porphyritic pyroxenite and a strongly foliated pyroxenite) show a depletion in Sr and Zr. The mineralized pyroxenite (sample 13VN107A03) shows enrichment of Ba and Sr, but depletion in Th, U and Nb.

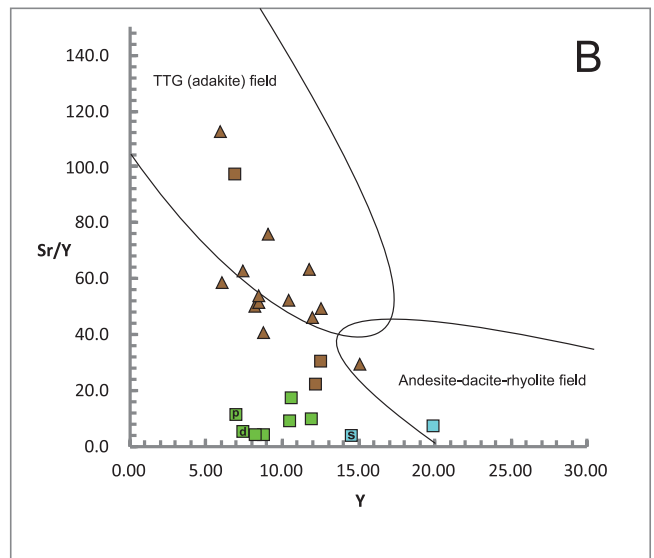
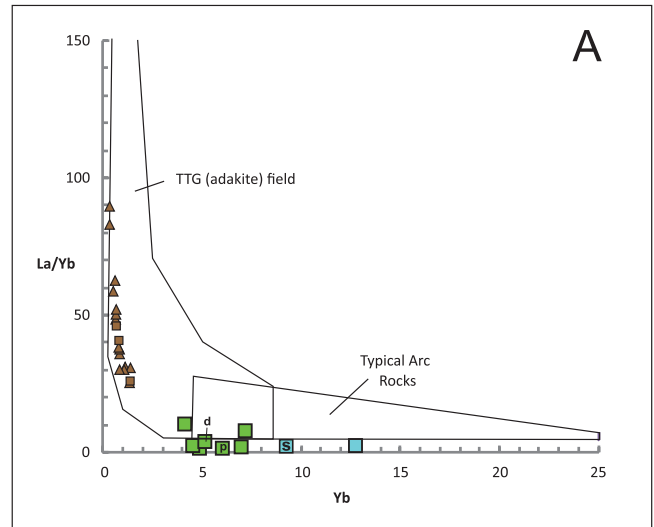


Figure 9. A) La/Yb vs Yb diagram discriminating TTG (adakite) and typical volcanic arc fields (Dummond and Defant, 1990). B) Sr/Y vs Y -diagram discriminating TTG (adakite) and normal andesite–dacite–rhyolite (Castillo, 2006). Symbols as in Figure 4.

Figure 11C shows the flat, very slightly light-REE-enriched profiles for the two gabbros. The gabbro sill exhibits a slight negative Eu anomaly. Figure 11D shows trace-element profiles of the two gabbro samples. Both have relatively flat multi-element profiles with variable Ba and small Nb troughs. The gabbro sill shows a pronounced depletion in Ti and slight Sr depletion, whereas the elements Ti, Zr and U are slightly depleted in the gabbro pluton.

The three tonalites have mutually similar rare-earth element profiles (Figure 11E) and multi-element profiles (Figure 11F). They are light-REE-enriched, have minor Eu spikes and exhibit saucer-shaped heavy-REE segments. The tonalities are enriched in the most incompatible elements

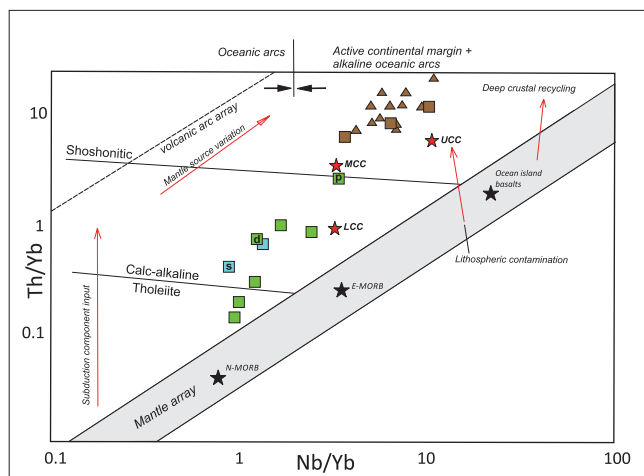


Figure 10. *Th/Yb vs Nb/Yb diagram illustrating the position of the mantle array, tholeiitic, calc-alkaline and shoshonitic fields and vectors for rocks enriched by input from a subduction component, crustal contamination and deep crustal recycling (after Pearce, 2008). Positions of average crustal values – LCC (lower continental crust), MCC (middle continental crust), UCC (upper continental crust) from Rudnick and Gao (2003). Symbols as in Figure 4.*

(Ba, Th, U), have Nb-Ta, Zr and Ti troughs and minor positive and negative anomalies for Sr. Percival *et al.* (2003) noted that the rare-earth element levels for rocks of the Desliens igneous suite are highest for the low silica tonalites (<60% SiO₂). The low silica tonalite from this study (60.3% SiO₂, sample 13VN085, Table 1) is slightly enriched in the LREE but has a lower HREE content compared to a tonalite with a higher silica content of 64.4% (Table 1). Rare-earth element contents are lowest for the high silica tonalite (66% SiO₂).

Summary of Litho-geochemistry

The ultramafic rocks, gabbro intrusions and the tonalites exhibit multi-element profiles that are typical of rocks generated in subduction environments, characterized by Nb and Ti troughs. These anomalies are a function of the transfer of Th and the LREE to the mantle source from fluids derived from the subducting slab (Pearce, 1983).

The major- and trace-element characteristics of the gabbro and ultramafic rocks indicate high MgO, Mg#, Cr and Ni and enrichment in both the compatible and incompatible elements. Extended trace-element and REE profiles indicate LREE-enrichment, negative Nb and Ti anomalies and weak to absent Eu anomalies. Percival *et al.* (2003) argued that these geochemical characteristics of the calc-alkaline intrusive rocks of the Desliens igneous suite indicate that they

preserve mantle signatures. A similar inference may be made with respect to the gabbro and ultramafic rocks based on LREE enrichment, depleted HREE, elevated Th contents with respect to the MORB array (Figure 10) and the overall high transition metal contents.

The position of the samples with respect to the MORB array in Figure 10 indicates that lithospheric or crustal contamination through subduction processes was likely a factor in the evolution of the gabbro and ultramafic rocks and the tonalitic rocks of the Desliens igneous suite. The inference of crustal contamination is supported, in part, by the presence of inherited zircon within tonalite of the suite as well as the presence of local garnet. The former are considered to have been derived from pre-metamorphic sedimentary rocks of the region, and the latter from local crustal rocks, in the marginal zones of some intrusions (Percival *et al.*, 2003).

IMPLICATIONS FOR THE PETROGENESIS OF ROCKS OF THE DESLIENS IGNEOUS SUITE AND GABBRO-ULTRAMAFIC ROCKS

Percival (1991a) and Percival *et al.* (2003) indicated that although the ultramafic units and rocks of the Desliens igneous suite have analogous field relations and similar textures and anhydrous assemblages, a lack of rocks having compositions intermediate between pyroxenite and diorite precluded a mutual relationship through crystal-liquid fractionation. In addition, rocks with compositions more mafic than diorite are very rare in TTG (adakitic) suites (Drummond and Defant, 1990). This observation does not necessarily negate a relationship through other petrogenetic processes such as variable degrees of fluid- and melt-related interactions and crustal input through subduction process. Percival *et al.* (2003) proposed the most likely setting for the formation of the suite was above a subducting, hot oceanic slab. This resulted in fluid-melt metasomatism of the overlying arc lithosphere in the hanging wall, and low degrees of partial melting in the mantle wedge. This was hypothesized to precede ridge-trench collision. The authors argued that a variety of processes may be responsible for producing the major- and trace-element characteristics of the suite, and that their high Mg#, Cr, Ni and light-REE enrichment may be explained by introducing variable amounts of slab-melt flux into the asthenospheric mantle source. Although a direct geochemical link between the calc-alkaline Desliens igneous suite and the ultramafic rocks with tholeiitic to arc-transitional affinity is not apparent, a similar scenario may be suggested for the formation of the gabbro and ultramafic rocks.

The influence of melt- and fluid-related enrichment and the effects of slab melting and continental contamination of the source rocks are investigated in Figure 12A and B. In the

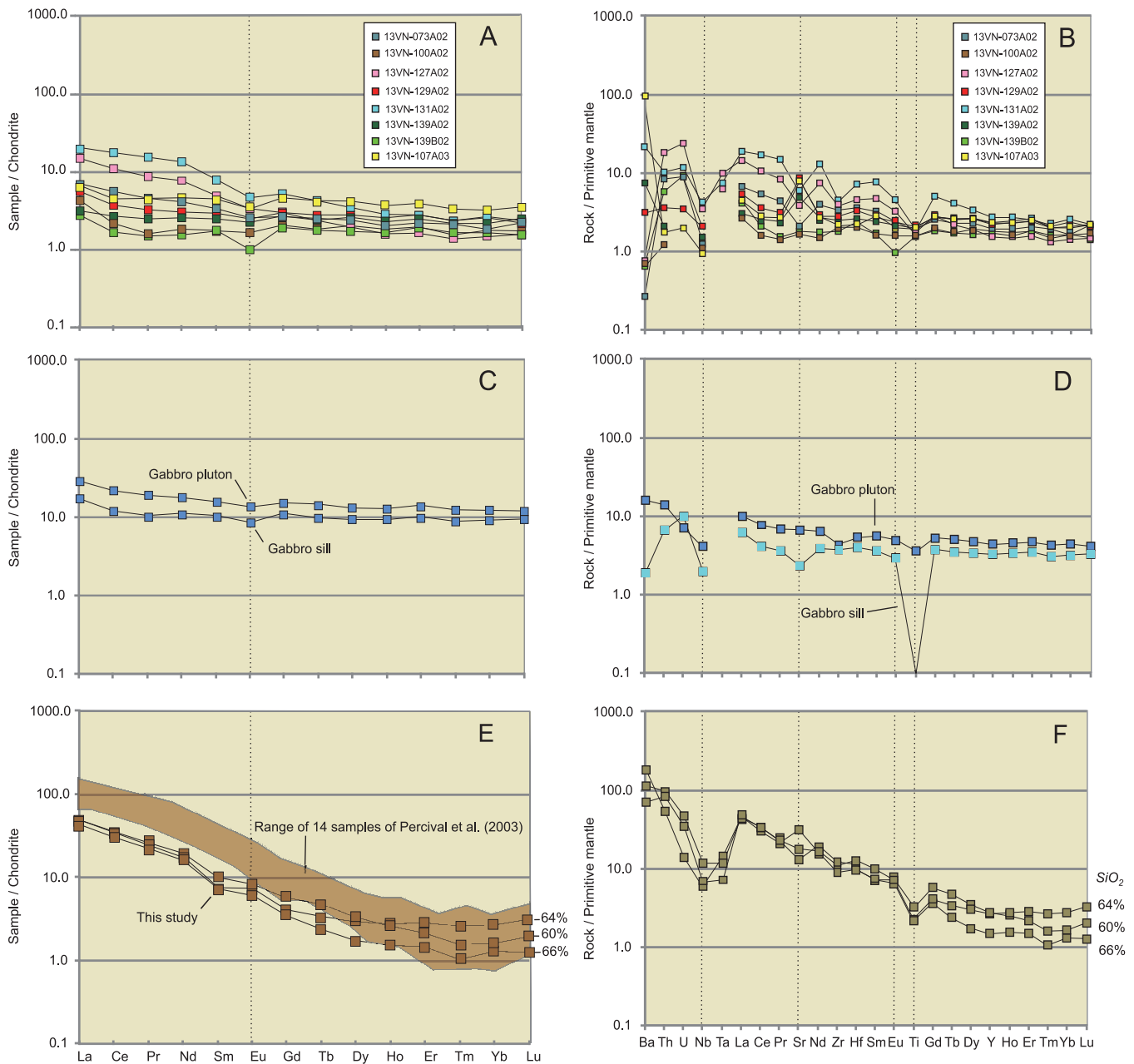


Figure 11. Chondrite-normalized REE (A, C and E) and primitive mantle-normalized multielement plots (B, D and F) for the rocks of the study area. Normalizing values are after Sun and McDonough (1989). Silica contents are noted for the three tonalites of this study in order to illustrate REE variation with respect to SiO₂ content.

Nb/Zr vs Th/Zr-diagram (Figure 12A: Kepezhinskas *et al.*, 1997) the gabbro, ultramafic rocks and the tonalites all have narrow ranges in Nb/Zr, plotting roughly parallel to the fluid-related enrichment trend. This suggests that fluid enrichment, likely through mantle metasomatism, may have had a significant effect on the source of the mafic-ultramafic rocks and the tonalitic units of the suite. Low Nb/Zr ratios implies that enrichment of their source through interaction with mantle melts may not have been important in the evolution of these rocks.

In the Th vs Nb/Th plot (Figure 12B; Zhao and Zhou, 2007), two contrasting trends are evident. The gabbro and ultramafic rocks exhibit a steep negative correlation of Nb/Th with Th, approximately paralleling the slab melt trend and suggesting that varying proportions of slab melt was involved in the formation of these rocks. The tonalitic rocks of the Desliens igneous suite, however, have very consistent low Nb/Th ratios that trend toward upper crust compositions (Rudnick and Gao, 2003). This observation suggests that the source of the tonalites was strongly influenced

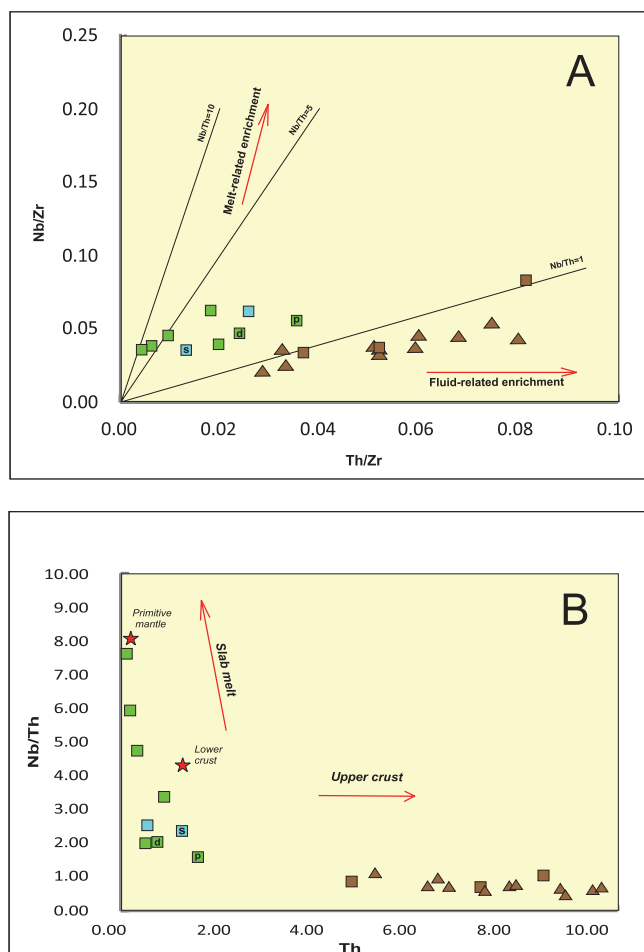


Figure 12. A) Nb/Zr vs Th/Zr–plot showing trends typical of fluid- and melt-related enrichment of mantle source rocks (Kepezhinskas *et al.*, 1997). B) Nb/Th vs Th plot illustrating effects of the addition of slab melt and continental crust to a mantle source (after Zhao and Zhou, 2007). Primitive mantle values after Sun and McDonough (1989).

by crustal input. The contrasting trends for the gabbroic and ultramafic rocks *versus* the tonalites indicate there may have been different amounts of slab melting, mantle source enrichment *via* fluids and crustal contamination in the evolution of the rocks of the region and their mutual relationship is equivocal.

The similarity in their field relationships with other units, their textures and bulk compositions indicate that the ultramafic rocks are likely a related suite of pre-tectonic cumulate rocks having transitional tholeiite–calc alkaline affinities. The two crosscutting ultramafic intrusions in the western study area have similar major- and trace-element characteristics perhaps suggesting that the smaller intrusion is a later phase of the larger sill and that these ultramafic rocks have a more complex evolution than previously recognized. Despite similar mineral assemblages and textures,

the contrasting field relationships (*i.e.*, a concordant sill compared to an irregular-shaped pluton) and differing bulk compositions suggest that the gabbro sill and pluton are not likely related and could represent different generations of intrusion. The gabbro sill, however, has a similar intrusive relationship and exhibits some major-, trace- and rare-earth element characteristics comparable to several ultramafic sills. The gabbro sill contains equivalent Ni, Cr and MgO has comparable Ti and Nb depletion, and similar REE abundances, suggesting similar mantle sources for the gabbro sill and the ultramafic rocks.

Additional geochemical analyses and precise geochronology of the gabbroic and ultramafic rocks, including a more comprehensive study of the individual components of the larger, layered ultramafic sills, are required to definitively evaluate the petrogenetic relationships of these rocks. Although gabbroic rocks are uncommon in the study area, analyses of other gabbroic sills and plutons in other parts of the Ashuanipi Complex would contribute to a better understanding of their relationship with the ultramafic rocks and if there is a petrogenetic association with the more calc-alkaline rocks of the Desliens igneous suite.

IMPLICATIONS FOR MINERAL POTENTIAL OF ROCKS OF THE REGION

Tonalite–trondhjemite–granodiorite suites or adakitic rocks have been genetically linked to the majority of the world’s Cu–Au mineralization (Mungall, 2002) and this association could be significant in terms of the mineral potential of the calc-alkaline granitoids of the Desliens igneous suite. Moritz and Chevè (1992) investigated gold mineralization hosted in iron formation rocks in the north-eastern Ashuanipi Complex and suggested that post-metamorphic mineralizing fluids acted as a transporting agent. They further proposed that these fluids may have been controlled by the lithology of the immediate wall rock and were distinct from “regional” fluids trapped in the metatexite and diatexite units. Although the source of the gold is unknown, Percival *et al.* (2003) suggested that the relatively high transition metal content of the rocks of the suite may indicate a potential for these rocks to host elevated gold.

The anhydrous nature of the Desliens igneous suite may limit the involvement of magmatic fluids as transporting agents. However, if local fluids can be sourced from hydrous wall rocks such as migmatitic metasedimentary gneiss or later granitoid intrusions, then these wall rocks may act as an important source of hydrothermal fluids for transporting sulphides along zones of structural weakness.

The east-southeast-striking fault in the southern study area that cuts through the rocks of the Desliens igneous suite may be a prospective area for mineralization (Figure 3).

Local syn-tectonic quartz veins cut tonalite to granodiorite gneiss along this fault zone (van Nostrand and Bradford, 2014) and could be a potential host for gold mineralization. Several northeast-striking lineaments that cross this fault may be late stage fractures or faults, also with a potential for fluid migration and metal deposition. Five slightly elevated gold-in-lake sediment values, ranging from 5.7 to 8.1 ppb Au, occur proximal to the junction of the southeast-striking fault and the strong northeast-striking lineament, immediately west of the ultramafic body, and may indicate possible gold mineralization in the tonalite intrusions (Unit At-gn, Figure 3).

In the study area, work related to economic mineralization is limited to cursory sampling of local gossan zones in foliated and gneissic granitoid rocks (tonalite to diorite composition) as part of industry and government surveys. Pyrrhotite, arsenopyrite, chalcopyrite and minor bornite occur as local disseminations in altered pyroxenite zones occurring along contacts with enclosing metasedimentary gneiss and diatexite. These have slightly elevated gold and base-metal values. One tonalite sample from this study returned a value of 6 ppb Au (sample 13VN076A02, Table 1). Despite the local occurrence of mineralization in these rocks, the overall elevated transition element contents (Percival *et al.*, 2003 and this study, Table 1) might indicate a potential for these rocks to either host or be a source of mineralization. Deposits would be associated primarily with lithological contacts, shear zones and faults where fluid mobility would be favourable.

Gabbroic and ultramafic rocks have the potential to contain two main base-metal deposit types: 1) primary magmatic Ni–Cu–(PGE) deposits and; 2) remobilized sulphide mineralization related to hydrothermal activity along local shear zones, faults and lithological contacts. A third, although probably less prospective type, are stratiform chromite deposits.

Arndt *et al.* (2005) divided primary magmatic deposits into three types, formed by segregation of immiscible sulphide liquids from mafic and ultramafic silicate magmas. Type I deposits form early in the crystallization history as massive and disseminated layers at or near the base of intrusions. Type II mineralization forms later in the crystallization history as stratabound layers with variable disseminated sulphide textures. Type III deposits form thin stratiform layers (reefs) during fractional crystallization of thick flows and sills. The main conditions required for the formation of Type I and II magmatic Ni–Cu–PGE deposits include: the production of large quantities of hot, primitive (mantle-compatible element fertile) magma, sulphur-undersaturation of the magmas during segregation and ascent, and assimilation of sulphur-rich crustal rocks to form and concentrate the sul-

phide minerals (Arndt *et al.*, op.cit.). Type III are low sulphur deposits and are more dependent on crystal fractionation and the formation of cumulate igneous layers.

In the study area, the movement of large quantities of magma may have been limited as most of the boudinaged sills are relatively small in dimension. However, as the intrusions were emplaced into metasedimentary rocks, the magma could have absorbed sufficient sulphur-bearing crustal material during segregation and ascent to form magmatic sulphide deposits. Alternatively, if these processes were not involved, low-sulphur Type III deposits may have formed in the thicker ultramafic sills.

Mineralization in the gabbroic and ultramafic rocks comprises sporadic disseminations in limonite-altered gossan zones and cm- to 10s of cm-wide, discontinuous layers and lenses having 1–4% sulphides. The main sulphide phases are pyrrhotite, chalcopyrite, arsenopyrite and minor bornite. Schofield (2014) identified pentlandite intergrown with pyrrhotite and chalcopyrite in the large sill (13VN127A02) in the southern study area (Figure 3). Schofield (*op. cit.*) also noted that the sulphides form dispersed, ovoid-shaped blebs perhaps suggesting a primary magmatic origin for the sulphides through the formation of immiscible droplets in a sulphur saturated magma. Most of the sulphide mineralization noted in the ultramafic rocks is associated primarily with strongly altered and sheared sill margins and along contacts of some individual cumulate layers. Because mineralization is apparently restricted to these settings, this suggests that remobilization of primary magmatic sulphides, possibly by movement of post-metamorphic fluids along zones of structural weakness, is the main potential deposit type in these rocks.

Investigation of the mafic and ultramafic rocks as potential host rocks to base and precious metal mineralization has only been carried out on a cursory basis. Thomas and Butler (1987), Dimmell (1989) and Graves (1992) reported local elevated values of Au, Ni, Cu and Cr from soil samples and from bedrock and boulder sampling of several gossan zones. Some of these were associated with altered mafic and ultramafic rocks. A value of 120 ppb Au was returned from a mafic boulder sampled near the large sill (13VN100A02) in the western study area (Figure 3: Thomas and Butler (1987) and Graves (*op. cit.*) reported slightly elevated values of 13 ppb Pd and 17 ppb Pt from a gossan in this sill. Percival (1987) reported an anomalous value of 70 ppb Pt from a sulphide-bearing zone at the base of the large ultramafic sill in the Pyroxenite Lake intrusion to the north of the study area (Figure 3). Detailed lake-sediment surveys (McConnell *et al.*, 1989 and McConnell, 2012) indicate elevated Au, Ni, Cr, Cu and V in areas underlain by some of the larger ultramafic sills in the western and southern parts of the study area.

Two of the unaltered pyroxenite samples and the gabbro sill from this study have slightly elevated gold values ranging from 10–12 ppb Au. The pyrrhotite-bearing pyroxenite yielded values of 11 ppb Au, 4560 ppm Cr, 4100 ppm Ti, 949 ppm Ni and 460 ppm Cu (sample 13VN107A03: Figure 3 and Table 1). Rare-earth element and multi-element plots for this mineralized sample (Figure 11A, B) indicate a strong enrichment in Ba and a weak addition of Sr, compared to the unaltered sills, otherwise element concentrations are very similar and show weak Nb, Th and Ti depletion, slight LREE enrichment and a flat HREE profile. The sample is also enriched in Rb (100 ppm, Table 1). The enrichment of the altered sill margin in Ba, Rb and to a lesser extent, Sr, would suggest the mineralization is associated with the addition of LILE-enriched fluids, probably derived from the adjacent migmatitic metasedimentary gneiss. The elevated contents of Cr, Cu, Ti and slightly elevated Au in the altered zone imply that some transition metals and gold were remobilized and concentrated by these fluids along the marginal zone of the intrusion.

Although the sills in the study area are not continuous, a few are 150–200 m thick, up to 1.5 km in strike length, and are coincident with intense magnetic highs (*see* Figure 4, van Nostrand and Bradford, 2014). Detailed study of all of these intrusions is necessary to evaluate their mineralization potential. Similar textures, in particular the presence of the characteristic coarse-grained pyroxene oikocryst-rich cumulate layers along with comparable field relations and bulk compositions support a petrogenetic link between the sills of the study area and the larger Pyroxenite Lake intrusion in adjacent Québec (Figure 3).

More detailed mapping and systematic geochemical sampling of the ultramafic sills and gabbroic intrusions would provide a better understanding of the origin of these rocks and whether they are mutually associated. Additional analyses of mineralized zones, particularly for PGE content, as well as ground-based electromagnetic geophysical surveys of these units to better define the extent of individual boudinaged sills and associated mineralization would provide a more comprehensive basis to evaluate the potential of these rocks to host Au, Ni, Cr, Cu, Ti and PGE deposits.

ACKNOWLEDGMENTS

Thanks go to Greg Dunning and Marina Schofield for discussions in the field and input in assessing the chemistry of some of the mafic and ultramafic rocks in the study area. Alana Hinchey and Hamish Sandeman reviewed earlier drafts of this report and are thanked for suggesting significant improvements.

REFERENCES

- Arndt, N., Lesher, C.M. and Czamanske, G.K.
2005: Mantle-derived magmas and magmatic Ni-Cu-(PGE) deposits. *Economic Geology*, 100th Anniversary Volume, pages 5-24.
- Beard, J.S.
1986: Characteristic mineralogy of arc-related cumulate gabbros: implications for the tectonic setting of gabbroic plutons and for andesite genesis. *Geology*, Volume 4, pages 848-851.
- Card, K.D. and Ciesielski, A.
1986: Subdivisions of the Superior Province of the Canadian Shield. *Geoscience Canada*, Volume 13, pages 5-13.
- Castillo, P.R.
2006: An overview of adakite petrogenesis. *Frontiers. Chinese Science Bulletin*, Volume 51, Number 3, pages 257-268.
- Chevè, S.R. and Brouillette, P.
1992: Reconnaissance géologique et métallogénique au NW de Shefferville, région du lac Weeks (1/2E) et de la Rivière Pailleraut (1/2W). *Territoire du Nouveau-Québec, ministère de l'Énergie et des Ressources, Québec*, 1 carte, 226 pages (MB92-12).
- Dimmell, P.
1989: First year assessment report on the Labrador Trough properties, Project 7418, western Labrador, Licences 258-265H, 269-276M and 289-292M, NTS 23J/2,3,6,7,10 and 11. *Corona Corporation*, 49 pages, GS# 23J/272.
- Drummond, M.S. and Defant, M.J.
1990: A model of trondhjemite-tonalite-dacite genesis and crustal growth via slab melting: Archean to modern comparisons. *Journal of Geophysical Research*, Volume 95, pages 503-521.
- Finch, C.
1998: Inductively coupled plasma-emission spectrometry (ICP-ES) at the Geochemical Laboratory. *In* Current Research. Government of Newfoundland and Labrador, Department of Mines and Energy, Geological Survey, Report 98-1, pages 179-193.
- Graves, G.
1992: First year assessment report on prospecting at

- Menihék Lake, License 383M, 386M and 398M, NTS 23J/6, 11. Noranda Exploration Company Limited, 74 pages.
- Hallberg, J.
1985: Geology and mineral deposits of the Leonora-Laverton area, northeastern Yilgarn Block, Western Australia. Hesperian Press, Perth, Western Australia, 140 pages.
- Irvine, T.N. and Baragar, W.R.A.
1971: A guide to the chemical classification of the common volcanic rocks. Canadian Journal of Earth Sciences, Volume 8, pages 523-548.
- James, D.T.
1997: Geology of the Archean Ashuanipi Complex, western Labrador. Government of Newfoundland and Labrador Department of Mines and Energy, Geological Survey, Report 97-2, 27 pages.
- Jensen, L.S.
1976: A new cation plot for classifying subalkalic volcanic rocks. Ministry of Natural Resources, Ontario Division of Mines, Miscellaneous Paper 66, 22 pages.
- Kepezhinskis, P., McDermott, F., Defant, M., Hochstaedter, A., Drummond, M.S., Hawdesworth, C.J., Koloskov, A., Maury, R.C. and Bellon, H.
1997: Trace element and Sr-Nd-Pb isotopic constraints on a three-component model of Kamchatka Arc petrogenesis. *Geochimica et Cosmochimica Acta.*, Volume 61, pages 577-600.
- Le Bas, M.J., Le Maitre, R.W., Streckeisen, A. and Zanettin, B.
1986: A chemical classification of volcanic rocks based on the total alkali silica diagram. *Journal of Petrology* Volume 27, Number 3, pages 745-750.
- McConnell, J.W.
2012: New ICP-ES geochemical data for regional Labrador lake-sediment and lake-water surveys. Government of Newfoundland and Labrador, Department of Natural Resources, Geological Survey, Open File LAB/1465, 25 pages.
- McConnell, J.W., Honarvar, P. and Whelan, G.
1989: Soil, rock and stream sediment surveys for gold mineralization in the Ashuanipi complex, western Labrador. Government of Newfoundland and Labrador, Geological Survey Branch, Open File LAB/0842, 136 pages.
- Middlemost, E.A.K.
1985: *Magmas and Magmatic Rocks. An Introduction to Igneous Petrology.* Longman, London, New York, 266 pages.
- Morisset, N.
1988: Metamorphism and geothermometry of a layered ultramafic sill in the Ashuanipi Complex, Superior Province, northern Québec. B.Sc. (Hons.) Thesis, Department of Geology, University of Ottawa, 92 pages.
- Moritz, R.P. and Chevè, S.R.
1992: Fluid inclusion studies of high-grade metamorphic rocks of the Ashuanipi Complex, eastern Superior Province: constraints on the retrograde P-T path and implications for gold metallogeny. *Canadian Journal of Earth Sciences*, Volume 29, pages 2309-2337.
- Mortensen, J.K. and Percival, J.A.
1987: Reconnaissance U-Pb zircon and monazite geochronology of the Lac Clairambault area, Ashuanipi complex, Québec. Geological Survey of Canada, Paper 87-2, pages 135-142.
- Mungall, J.E.
2002: Roasting the mantle: Slab melting and the genesis of major Au and Cu-rich Cu deposits. *Geology*, Volume 30, Number 10, pages 915-918.
- Pearce, J.A.
1983: Role of sub-continental lithosphere in magma genesis at active continental margins. *In Continental Basalts and Mantle Xenoliths.* Edited by C.J. Hawkesworth and M.J. Norrly. Shivan Nantwich, U.K., pages 230-249.
- 2008: Geochemical fingerprinting of oceanic basalts with applications to ophiolite classification and the search for Archean oceanic crust. *Lithos*, Volume 100, pages 14-48.
- Percival, J.A.
1987: Geology of the Ashuanipi granulite complex in the Schefferville area, Québec. *In Current Research, Part A.* Geological Survey of Canada, Paper 87-1A, pages 1-10.
- 1991a: Orthopyroxene-poikilitic tonalites of the Desliens igneous suite, Ashuanipi granulite complex, Labrador-Québec, Canada. *Canadian Journal of Earth Sciences*, Volume 28, pages 743-753.

- 1991b: Granulite facies metamorphism and crustal magmatism in the Ashuanipi complex, Québec-Labrador, Canada. *Journal of Petrology*, Volume 32, pages 1261-1297.
- 1993: Geology, Ashuanipi Complex, Schefferville area, Newfoundland–Québec. Geological Survey of Canada, Map 1785A, scale 1:125 000.
- Percival, J.A. and Girard, R.
1988: Structural character and history of the Ashuanipi Complex in the Shefferville area, Québec-Labrador. *In* Current Research, Part C. Geological Survey of Canada, Paper 88-1C, pages 51-60.
- Percival, J.A., Mortensen, J.K. and Roddick, J.C.M.
1988: Evolution of the Ashuanipi granulite complex: conventional and ion probe U-Pb data. Geological Association of Canada – Mineralogical Association of Canada – Canadian Society of Petroleum Geologists, Joint Annual Meeting, Program with Abstracts, Volume 13, page A97.
- Percival, J.A., Stern, R.A. and Rayner, N.
2003: Archean adakites from the Ashuanipi Complex, eastern Superior Province, Canada: geochemistry, geochronology and tectonic significance. *Contributions to Mineralogy and Petrology*, Volume 145, pages 265-280.
- Ross, P.S. and Bedard, J.H.
2009: Magmatic affinity of modern and ancient subalkaline volcanic rocks determined from trace-element discriminant diagrams. *Canadian Journal of Earth Sciences*, Volume 46, pages 823-839.
- Rudnick, R.L. and Gao, S.
2003: Composition of the continental crust. *In* Treatise on Geochemistry, Geochemistry of the Crust, Volume 2. Edited by R.L. Rudnick. Elsevier, Amsterdam, pages 1-64.
- Schofield, M.
2014: Petrology of a layered ultramafic to mafic intrusion: Ashuanipi Complex, Labrador. B.Sc. (Hons) thesis, 85 pages, Memorial University of Newfoundland and Labrador, Department of Earth Sciences.
- Sun, S.S. and McDonough, W.F.
1989: Chemical and isotopic systematics of oceanic basalts: implications for mantle composition and processes. *In* Magmatism in the Ocean Basins. Edited by A.D. Saunders and M.J. Norry. Geological Society of London Special Publications, Volume 42, pages 313-345.
- Thomas, A. and Butler, J.
1987: Gold reconnaissance in the Archean Ashuanipi Complex of western Labrador. *In* Current Research. Newfoundland Department of Mines and Energy, Mineral Development Division, Report 87-1, pages 237-255.
- van Nostrand, T. and Bradford, W.
2014: Geology of the northeastern Ashuanipi Complex, western Labrador (parts of NTS 1:50 000-scale map areas 23J/6, 7, 11,14 and 23O/3) *In* Current Research. Newfoundland and Labrador Department of Natural Resources, Geological Survey, Report 14-1, pages 189-216.
- Winchester, J.A. and Floyd, P.A.
1977: Geochemical discrimination of different magma series and their differentiation products using immobile elements. *Chemical Geology*, Volume 20, pages 325-343.
- Zhao, G.C. and Zhao, M.F.
2007: Geochemistry of Neoproterozoic mafic intrusions in the Panzihua district (Sichuan Province, SW China): Implications for subduction related metasomatism in the upper mantle. *Precambrian Research*, Volume 152, pages 27-47.

APPENDIX

The following are brief descriptions of tonalite, gabbro and ultramafic rock samples collected from the study area. Locations below are referenced in UTM coordinates, NAD 27, Zone 19 and are indicated on Figure 3. The descriptions and locations of samples analyzed by Percival *et al.* (2003) and Morisett (1988) are not included.

Ultramafic Samples

13VN073A02 (UTM-620907E / 6039286N)

Dark-weathering, fine- to medium-grained, strongly foliated homogeneous pyroxenite sill margin. Contains 80–85% ortho- and clinopyroxene, 5% olivine, 5% plagioclase+amphibole.

13VN100A02 (UTM-617989E / 6045341N)

Dark-weathering, medium-grained, strongly foliated, homogenous pyroxenite containing 85–90% orthopyroxene, 5% clinopyroxene and 5% combined olivine, plagioclase and magnetite.

13VN107A03 (UTM-623116E / 6040172N)

Fine- to medium-grained, brown-weathering, locally layered, 15-m-thick ultramafic sill consisting primarily of pyroxenite with local websterite. The sill intrudes well-banded migmatitic granodiorite gneiss. The sample was collected from a 1-m-wide limonite-altered gossan zone in pyroxenite along the sill–gneiss contact and contains 1–4% disseminated pyrrhotite and trace chalcopyrite.

13VN127A02 (UTM-623822E / 6034048N)

Black- to grey-weathering, coarse-grained porphyritic pyroxenite varying locally to websterite. Contains partially altered relict orthopyroxene and clinopyroxene igneous phenocrysts up to 2.5 cm in diameter with a matrix of 80% pyroxene, 10% olivine, 5–10% plagioclase+amphibole.

13VN129A02 (UTM-628667E/6029491N)

Grey- to black-weathering, medium-grained, strongly foliated pyroxenite. The rock consists of 90% ortho- and clinopyroxene and 10% combined olivine, amphibole and minor plagioclase and exhibits a very weak compositional layering.

13VN131A02 (UTM-624913E / 6034524N)

Black- to grey-weathering, medium-grained, strongly foliated pyroxenite grading to websterite with 5–10% olivine. Rock contains orthopyroxene, olivine, biotite, amphibole and magnetite.

13VN139A02 (UTM-617614E / 6045105N)

Medium- to coarse-grained, homogeneous, moderate to strongly foliated pyroxenite. This is the primary rock type of the large, northeast-striking sill in the western study area. Contains 85–90% orthopyroxene+clinopyroxene, less than 5% olivine and minor spinel and magnetite.

13VN139B02 (UTM-617614E / 6045105N)

Fine-grained, brown-weathering, weakly foliated pyroxenite varying locally to websterite, which truncates the strong fabric in the coarse-grained pyroxenite described above (VN-139A02) and appears to be a separate, later dyke or minor intrusion.

Gabbro Samples

13VN074A02 (UTM-622716E / 6047677N)

Medium-grained, massive to weakly foliated gabbro grading locally to meladiorite. Rock consists of plagioclase, clinopyroxene, orthopyroxene, amphibole and minor magnetite.

13VN202A02 (UTM-615928E / 6050709N)

Medium-grained, grey-green-weathering, moderately foliated concordant gabbro sill intruding well-banded metasedimentary gneiss. The contact of the gneiss and gabbro is locally marked by local gossan zones. The sampled sill margin is melagabbroic

in composition and consists of 65% ortho- and clinopyroxene, 10–15% plagioclase, 10% amphibole+magnetite. The gabbro is slightly less mafic in the interior of the sill.

Tonalite Samples

13VN045A02 (UTM-641783E / 6041063N)

Medium- to fine-grained, well-banded, migmatitic garnet+orthopyroxene+biotite tonalite gneiss. The sample has a similar texture to that shown in Plate 2.

13VN076A02 (UTM-620404E / 6045308N)

Medium-grained, grey-weathering, massive to weakly foliated tonalite with 1–2 cm anhedral orthopyroxene grains, interpreted as relict igneous oikocrysts. Also contains plagioclase, biotite and minor magnetite, and the sample has a similar texture to that shown in Plate 1.

13VN085A02 (UTM-620076E / 6042654N)

Grey-weathering, strongly foliated, medium- to coarse-grained plagioclase+garnet+orthopyroxene+biotite+magnetite tonalite.